

Boundary-free scaling calculation of the time-dependent Schrödinger equation for laser-atom interactions

Z. X. Zhao, B. D. Esry, and C. D. Lin

Department of Physics, Kansas State University, Manhattan, Kansas 66506-2601

(Received 26 June 2001; published 3 January 2002)

The time-dependent Schrödinger equation for atoms in an intense laser field is solved in scaled coordinates. Starting with the time propagation of a free particle, we show that scaling removes the spreading and rapid phase variation of a wave packet. By solving the one-dimensional model atom in an intense laser field, we show that stable numerical results are best calculated in the acceleration gauge using scaled coordinates. The wave function thus calculated has the least oscillations and does not spread at large time so that there is no need to introduce absorbers at the boundaries. We show the method is suitable for calculations at any laser field strength. We also show that the scaling method permits propagation to large times thus revealing above threshold ionization structure directly in the wave function.

DOI: 10.1103/PhysRevA.65.023402

PACS number(s): 32.80.Rm, 32.80.Fb, 42.50.Hz

I. INTRODUCTION

The interaction of intense lasers with atoms has attracted considerable interest both experimentally and theoretically in recent years [1]. In an intense laser field, an atom can be ionized by processes such as multiphoton ionization [2] or by tunneling ionization [3]. Other phenomena such as above threshold ionization (ATI) [4,5] and harmonic generation (HG) [6,7] are also well known. The HG process is of particular interest since it may lead to new sources of coherent short wavelength light.

For laser intensities above about $10^{13} \text{ W cm}^{-2}$, perturbation theories can no longer be used to describe the laser-atom interactions. In the past, various nonperturbative approaches have been developed. One commonly used method is Floquet theory [8,9] and its generalization to the many-electron case in the form of the R -matrix Floquet method [10]. However, the method is not convenient for short laser pulses since it presumes a cw laser. The more common approaches for short laser pulses are based on solving the time-dependent Schrödinger equation either directly on numerical grids or in a basis set. In the basis-set approach, basis functions have been chosen to be the field-free atomic eigenstates [11,12], Volkov states [13], and others [14]. The resulting first-order time-dependent equations are solved by direct numerical integration or by using a fitting method [15]. Grid methods have included finite differences [16–19], discrete variable representation [20], finite elements [21], and B splines [22].

In the time-dependent approach, the goal is to obtain an accurate wave function for the electron throughout the duration of the laser pulse. This time-dependent wave function should describe not only the bound excited states, but also the continuum states representing the ionized electrons. When the calculation is carried out using basis functions, the continuum states are often represented by some set of pseudostates. When the calculation is carried out on a grid, the grides have to be confined to a box of finite size. Neither approach allows the continuum electrons to escape to infinity, and reflections from these artificial boundaries may result in unphysical interference. Although it is possible to enlarge

the box or basis set at a given time so that the wave function does not reach the boundary, or to introduce *ad hoc* absorbers near the boundaries, these approaches are inherently limited and should be used with care in intense fields where fast electrons are generated, and for long laser pulses where the propagation time is necessarily large.

The inherent limitations of representing a time-dependent continuum wave function by a finite basis or grid are apparent even for a freely propagating wave packet. Consider the well-known example of a Gaussian wave packet traveling with a group velocity k_0 . As time evolves, the wave packet will spread and at the same time acquire a rapidly increasing phase. The sharper the wave packet is initially, the larger and faster is the spreading. One way to avoid this spreading is to calculate the momentum wave function directly. In momentum space, the wave function is always localized and does not spread with time unless there is an external field. This is the approach taken by Sidky and Lin for treating impact ionization in ion-atom collisions [23]. Another approach is to use a scaled coordinate system. The scaled coordinate is chosen by scaling the spatial coordinate according to $\xi = x/R(t)$, where $R(t)$ is chosen arbitrary except it is set to approach γt at large times with γ a constant with units of velocity. Thus, in the scaled coordinate, the electron wave packet is stationary and does not expand with time. As shown by Sidky and Esry [24], in the scaled coordinates the rapid phase increase with time at large x is also removed, leaving a scaled, time-dependent wave function that varies slowly in both time and space. The scaling approach thus achieves the goals of the momentum-space approach *and* removes the rapid phase variation. Such functions are much easier to calculate numerically.

The two approaches mentioned in the previous paragraphs are designed specifically to treat the continuum wave function. In typical collision systems, however, there are also bound states to deal with. Solving the time-dependent Schrödinger equation entirely in momentum space would require the solution of an integro-differential equation, where the kernel involving the interaction potential is difficult to evaluate, if not impossible. Sidky and Lin circumvented this dif-

faculty by solving the time-dependent equation in coordinate space even though the wave functions are expanded in momentum-space-basis splines. In the scaled coordinate approach, the price to be paid for the simplification of the continuum wave function is that the bound states shrink with time. A flexible numerical representation is thus required, but no other difficulties result. In Sidky and Esry, a short-range model potential that could support only one bound state was examined. In the present paper, the scaled coordinate approach is applied to a one-dimensional soft-Coulomb potential in a laser field. We will show that the existence of many bound states does not pose any practical computational problems and that the scaled wave functions are indeed much smoother, thus making the method applicable for any field strengths and for propagation to very long times.

II. THEORETICAL METHODS

A. One-dimensional model atom

To illustrate the scaling method, we will perform calculations on a one-dimensional (1D) soft-Coulomb potential [17]

$$V(x) = -\frac{1}{\sqrt{1+x^2}}. \quad (1)$$

Just as for the three-dimensional case, this potential supports an infinite number of bound states. The ground state and the first excited state have energies of -0.669 and -0.275 a.u., respectively (we will use atomic units hereafter unless otherwise indicated). We choose a smooth turn on a cw laser

$$E(t) = \begin{cases} E_0 \sin^2\left(\frac{\pi t}{6T}\right) \sin(\omega t), & 0 \leq t \leq 3T \\ E_0 \sin \omega t, & t \geq 3T \end{cases} \quad (2)$$

where ω , E_0 , and T are the frequency, amplitude, and period of the laser field, respectively. Within the dipole approximation, the time-dependent Schrödinger equation in the length gauge is given by

$$i \frac{\partial \Psi_L(x,t)}{\partial t} = \left[\frac{p^2}{2m} - qEx + V(x) \right] \Psi_L(x,t), \quad (3)$$

where m is the mass of the electron, $q = -e$ is the electronic charge, and p is the momentum.

B. Scaling scheme

Following Sidky and Esry, the scaled coordinate is defined by

$$\xi = \frac{x}{R(t)}, \quad (4)$$

and the transformed, scaled wave function $\Psi^S(\xi, t)$ is given by

$$\Psi^S(\xi, t) = \sqrt{R} e^{-i\beta\xi^2} \Psi(x, t). \quad (5)$$

The superscript S is used to denote the scaled wave function, and the parameter β is

$$\beta = \frac{1}{2} mR \frac{dR}{dt}. \quad (6)$$

While the functional form of $R(t)$ is arbitrary, it should be chosen so that $R \rightarrow \gamma t$ at large t , with γ being a constant with units of velocity, in order to make the wave packet stationary. The time-dependent Schrödinger equation (TDSE) for $\Psi^S(\xi, t)$ is

$$i \frac{\partial \Psi^S(\xi, t)}{\partial t} = \left[-\frac{1}{2mR^2} \frac{\partial^2}{\partial \xi^2} - qRE\xi + V(R\xi) + \frac{1}{2} mR \frac{d^2R}{dt^2} \xi^2 \right] \Psi^S(\xi, t). \quad (7)$$

To illustrate how the scaling works, consider a one-dimensional Gaussian electronic wave packet with velocity k_0 and width a at time $t=0$ a.u. This wave packet will freely evolve as

$$\Psi(x, t) = \Phi(x, t) e^{i\varphi(x, t)}, \quad (8)$$

where the amplitude is given by [25]

$$|\Phi(x, t)|^2 = h(t) \exp\left[-\frac{(x-k_0t)^2}{w^2(t)}\right] \quad (9)$$

with

$$h(t) = \left[\frac{2a^2}{\pi(a^4 + 4t^2)} \right]^{1/2},$$

$$w(t) = \left(\frac{a^4 + 4t^2}{2a^2} \right)^{1/2}.$$

The center of the wave packet is thus moving with velocity k_0 and is spreading with time. The phase factor $\varphi(x, t)$ is given by

$$\varphi(x, t) = \frac{1}{2} \tan^{-1}\left(\frac{2t}{a^2}\right) + k_0x - \frac{1}{2} k_0^2 t + \frac{2t(x-k_0t)^2}{a^4 + 4t^2}, \quad (10)$$

and approaches

$$\frac{\pi}{4} + \frac{2tx^2}{a^4 + 4t^2}$$

at large times. This phase becomes linear in time at large t and depends quadratically on x , leading to rapid oscillations in the wave packet.

In contrast, using Eq. (5) and $R \rightarrow \gamma t$, the asymptotic form of the scaled wave function in the scaled coordinate is

$$\Psi^S(\xi) = \left[\frac{a^2 \gamma^2}{2\pi} \right]^{1/4} \exp\left[-\frac{a^2 \gamma^2}{4} \left(\xi - \frac{k_0}{\gamma}\right)^2\right] e^{i\pi/4}. \quad (11)$$

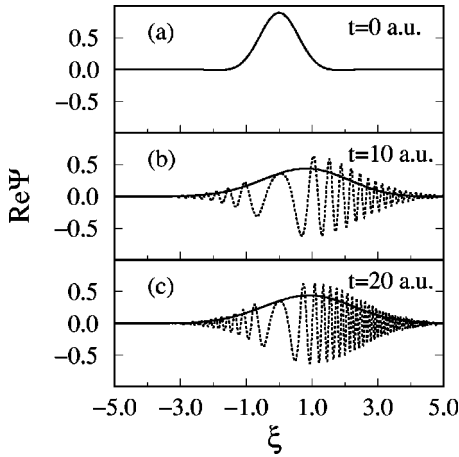


FIG. 1. Time evolution of a free wave packet. Only the real part of the wave function is shown. At $t=0$ a.u., the Gaussian wave packet has a width of 1 a.u. and is traveling to the right with a velocity of 1 a.u. The dashed line is for the real wave function and the solid line is for the scaled wave function showing that the latter has many fewer oscillations. The abscissa is the scaled coordinate. The scaling parameter is $R(t) = \sqrt{1+t^2}$ for positive t .

The scaled wave packet is thus *time independent* in the limit of large times. It is centered at $\xi = k_0/\gamma$, fixed in width, and has no rapid oscillations. Clearly such a function is much easier to calculate numerically than the original unscaled function.

As an illustration, we show in Fig. 1 the free propagation of a Gaussian wave packet. The velocity of the wave packet is 1 a.u. and its width is 1 a.u. at $t=0$. The real part of the wave function at $t=0, 10$, and 20 a.u. are plotted. The solid lines denote the scaled wave function; and the dotted lines, the weighted unscaled function $\sqrt{R}\Psi(R\xi, t)$. The abscissa is the scaled coordinate ξ , with the scaling parameter $R(t) = \sqrt{1+t^2}$ for $t \geq 0$. Several features of the scaling method are well illustrated here. First, the “real” wave function oscillates much more rapidly than the scaled function, and the differences grow with time as shown in the progression from curve (b) to (c). Second, in the scaled coordinates, the wave packet simply moves from $\xi=0$ to 1 as time goes from 0 to ∞ . Already at $t=10$ a.u. the wave packet has essentially reached its asymptotic position. Third, the width of the scaled wave packet has also nearly reached its asymptotic value at $t=10$ a.u., and has the manageable value $\Delta\xi \approx 2.5$. The real wave packet is 10 times bigger at $t=10$ a.u., and 20 times at $t=20$ a.u. In this example, the time evolution of the unscaled wave function is known analytically. If we were to obtain this oscillating function by direct numerical integration, it would clearly be a more challenging task.

The above example is for a freely propagating wave packet. In laser-atom interactions, the wave function of an ionized electron still under the influence of the laser field undergoes complicated evolution due to the quiver motion. This field-induced acceleration leads to oscillations of the wave function that are not removed by the scaling transformation since the latter accounts only for motion of a constant velocity wave packet. We will show in the following section how the quiver motion can also be analytically described.

C. Gauge transformations

It is well known that the wave function of a free electron in a cw laser field can be simplified by transforming from the length gauge to the acceleration gauge:

$$\Psi_L = \exp\left(-i\frac{q}{c}Ax\right) \exp(ip\alpha - i\mu) \Psi_A, \quad (12)$$

where

$$A(t) = A(0) - c \int_0^t E dt',$$

$$\alpha(t) = \alpha(0) + \frac{q}{c} \int_0^t A dt',$$

$$\mu(t) = \mu(0) + \frac{q^2}{2c^2} \int_0^t A^2 dt'. \quad (13)$$

This transformation can be easily understood classically. In the classical description, the motion of an electron is characterized by its position and velocity (x, v) . When the laser field is applied, these change to $[x - \alpha, v + (q/c)A]$. By shifting the center of (x, v) from $(0, 0)$ to $[\alpha, -(q/c)A]$, the effects of the laser field is removed, and the electron in this frame can be treated as freely propagating. This reference frame is called the Kramers-Henneberger (KH) frame, and the wave function is said to be in the acceleration gauge. We will use the terms KH frame and “acceleration gauge” interchangeably in the following. In the KH frame, the TDSE becomes

$$i \frac{\partial \Psi_A(x, t)}{\partial t} = \left[\frac{p^2}{2m} + V(x - \alpha) \right] \Psi_A(x, t). \quad (14)$$

In scaled coordinates for the 1D problem, it is given by

$$i \frac{\partial \Psi_A^S(\xi, t)}{\partial t} = \left[-\frac{1}{2mR^2} \frac{\partial^2}{\partial \xi^2} + V(R\xi - \alpha) + \frac{1}{2} mR \frac{d^2 R}{dt^2} \xi^2 \right] \Psi_A^S(\xi, t). \quad (15)$$

In the absence of the potential $V(x)$, the solution of Eq. (14) is a plane wave. By transforming to the length gauge through Eq. (12), we obtain the usual Volkov state that describes a free particle in a laser field.

Further insight into the effects of using the scaling approach can be obtained by considering the time evolution of an initial Gaussian wave packet (as in Fig. 1) in a laser field $E = \sin \omega t$ using the acceleration gauge. The time-dependent wave function can be obtained analytically even for this case. In the KH frame, the evolution of the Gaussian wave packet is given by the familiar free-particle result. To obtain the wave function in the length gauge, the gauge transformation in Eq. (12) can be applied to the KH frame wave function. Note that this is most straightforwardly accomplished by writing the Gaussian in terms of its Fourier components. The real part of the wave function in the scaled coordinate

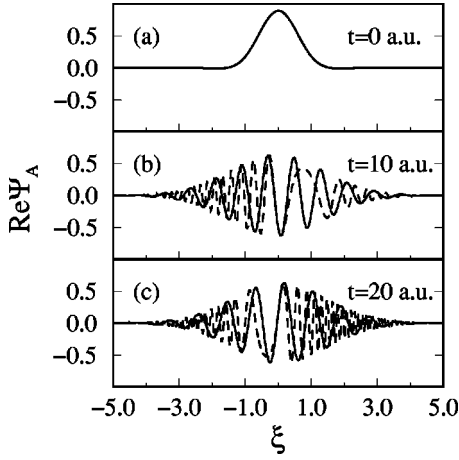


FIG. 2. Time evolution of the initial Gaussian wave packet of Fig. 1 in a cw laser field $E = \sin \omega t$. The solid line is for the scaled wave function and the dashed line is for the real wave function. The wave functions are in the length gauge, and only the real part is shown.

and in the real coordinate are compared in Fig. 2 at $t=0, 10,$ and 20 a.u. Even though the wave function is oscillatory in the scaled coordinate, the oscillation is still much slower than in the real-space wave function. The combination of acceleration gauge plus scaled coordinates thus accounts analytically for both the acceleration due to the laser and the constant-velocity free-particle propagation. The numerical simplifications that result are further examined below using a more realistic soft-Coulomb potential.

To integrate Eq. (15), we need the initial state in the acceleration gauge. It is obtained from the transformation

$$\Psi_A(x,0) = \exp[-ip\alpha(0) + t\mu(0)] \exp[i(q/c)A(0)x] \Psi_L(x,0). \quad (16)$$

At first glance, the choice $A(0) = \alpha(0) = \mu(0) = 0$ appears desirable since it would make the two functions identical at $t=0$. Such a choice, however, would result in a drift term, i.e., a term in $\alpha(t)$ linear in t that would carry the center of the potential away from $\xi=0$. Since we need a fine numerical mesh near the nucleus to account for the shrinking bound states, it is more efficient to choose the initial $A(0)$ so that the nucleus does not drift. With the laser field turn on given by Eq. (2), we found that $A(0) = -E_0/35\omega$ and $\alpha(0) = 0$ gives the desired transformation. Thus, in the scaled KH frame, the center of the soft-Coulomb potential follows the oscillating $\alpha(t)$ function with an amplitude of this oscillation decreases with time as $1/R$. Since the bound states move with the oscillating center, we need to use a fine spatial grid over the whole range of motion.

Once the time-dependent wave function is obtained, we can calculate the ATI spectrum by projecting it onto the continuum states of the field-free 1D atom. If $\Phi^c(x)$ is one of these continuum states, then the ATI spectrum can be calculated from the amplitude in the length gauge,

$$\begin{aligned} \langle \Phi^c(x) | \Psi_L(x,t) \rangle &= \langle \Phi^c(x) | e^{-i(q/c)Ax} e^{ip\alpha - i\mu} | \Psi_A(x,t) \rangle \\ &= \langle e^{-ip\alpha} \Phi^c(x) | e^{i(q/c)Ax} \exp[(q/c)A\alpha - i\mu] | \Psi_A(x,t) \rangle. \end{aligned} \quad (17)$$

In this expression, we have used the result

$$e^{-ip\alpha} e^{-i(q/c)Ax} e^{ip\alpha} = e^{-i(q/c)Ax} e^{i(q/c)A\alpha}, \quad (18)$$

which is obtained from the well-known formula

$$e^P Q e^{-P} = Q + [P, Q] + \frac{[P, [P, Q]]}{2!} + \dots \quad (19)$$

by letting $P = -ip\alpha$, $Q = e^{e^{i(q/c)Ax}}$. Thus, the projection in terms of scaled wave functions in the KH frame is given by

$$\langle e^{-ip\alpha} \sqrt{R} \Phi^c(R\xi) | \exp[-i(q/c)A(R\xi - \alpha)] | e^{i\beta\xi^2} \Psi_A^S(\xi, t) \rangle. \quad (20)$$

The function on the left side is most conveniently obtained by solving the ‘‘shifted’’ Schrödinger equation

$$\left[-\frac{1}{2mR^2} \frac{d^2}{d\xi^2} + V(R\xi - \alpha) \right] \psi = E_c \psi, \quad (21)$$

where

$$\psi = e^{-ip\alpha} \sqrt{R} \Phi^c(R\xi).$$

In our calculation, the range of ξ was normally chosen between -17 and $+17$. The solution of the above equation thus gives a set of pseudostates that represent the continuum. The distribution of pseudostates is dense enough to extract the ATI spectrum.

III. NUMERICAL RESULTS AND DISCUSSION

A. Wave functions in scaled coordinates

We now consider the solution of the 1D soft-Coulomb problem in a laser field to illustrate the advantages of performing calculations using scaled coordinates. We will focus on the strong field regime, where the challenge to the numerical method is most severe. In all the calculations, the lasers are turned on smoothly in three cycles as described in Eq. (2), and the electron is initially in the ground state. In the first calculation, we choose $\omega = 0.5193$ a.u. (or a period of 12.1 a.u.) and $E_0 = 1$ a.u. The scaling is applied starting at $t = 10$ a.u., and the scaling function $R(t) = \sqrt{1 + 0.04t(t-10)^2}$ for $t \geq 10$ a.u. No scaling was employed before $t = 10$ a.u., i.e., $R = 1$. The wave functions are calculated by integrating the TDSE in scaled coordinates using B splines in a Crank-Nicholson-like propagation scheme. The wave functions in real coordinates are obtained from Eq. (5).

In solving the time-dependent wave functions in the scaled coordinates, the range of ξ is chosen to make sure that it is large enough to enclose the scaled wave function at all times. The range, of course, depends on the scaling parameter $R(t)$ chosen. The grid points and the range stay fixed

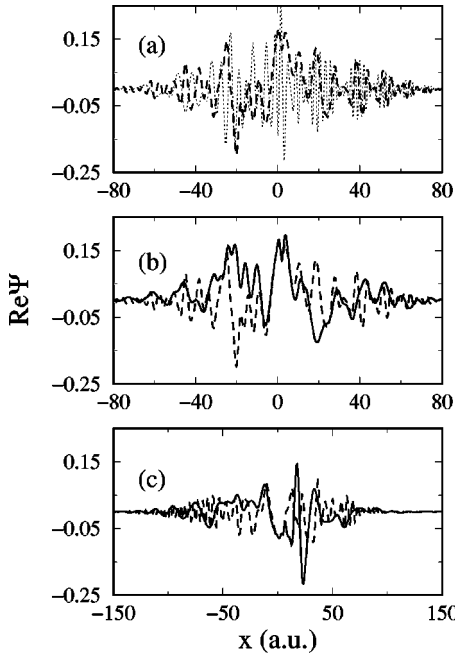


FIG. 3. In (a), comparison of the wave functions in length gauge (dotted line) and in acceleration gauge (dashed line). No scaling was used. Shown are the real part of the wave functions with $E_0 = 1$ a.u. and $\omega = 0.5193$ a.u. In (b), comparison of real wave function (dashed line) and the scaled wave function (solid line) in the acceleration gauge. Laser parameters are as in (a). Panel (c) is the same as (b) except that the laser field has strength $E_0 = 4$ a.u.

during the time integration. Since the bound states shrink with time, finer meshes are used for the region near the force center.

We first compare the wave functions in the acceleration gauge and in the length gauge without scaling at $t = 60$ a.u. The real parts of the wave functions are shown in Fig. 3(a). Clearly the oscillation in the length gauge is much more rapid except in the outer region, where they are comparable. It follows that the acceleration gauge has numerical advantages. A rapidly oscillating function not only requires more spatial grid points for accurate representation, but also smaller time steps.

The wave function in the acceleration gauge becomes even simpler in the scaling approach. Comparing the real part of the two functions in Fig. 3(b), the scaled wave function is clearly smoother and thus easier to compute directly. In fact, the unscaled wave function was obtained from the computed scaled wave function using Eq. (5).

We next consider a laser with the same frequency but with the higher field of $E_0 = 4$ a.u. In Fig. 3(c), we show the real part of the wave function at $t = 60$ a.u., again in the acceleration gauge. The scaling parameter is chosen as $R(t) = \sqrt{1 + 4(t-1)^2}$ for $t \geq 1$ a.u. The scaling must be started earlier and have a large γ due to the fast ionized electron. Without scaling, the wave function oscillates rapidly. Using scaling, the number of oscillations is substantially reduced, showing the merit of the scaled coordinates.

At field strengths of 1 and 4 a.u., the electron is readily ionized. In Fig. 4, we show the calculated ionization prob-

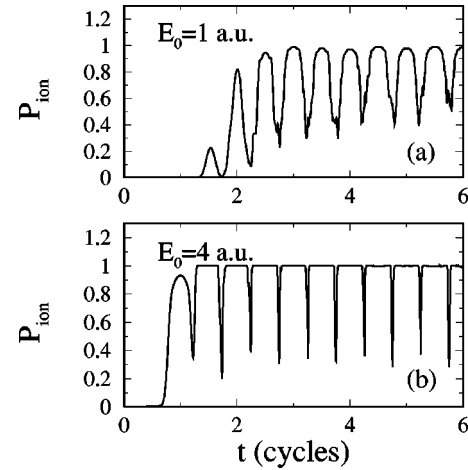


FIG. 4. Total ionization probabilities vs time for $\omega = 0.5193$ a.u.: (a) $E_0 = 1$ a.u. and (b) $E_0 = 4$ a.u.

ability vs time. The ionization probability oscillates with the laser period, with sharp minima at times of one quarter and three quarter cycles. Away from the minima, at these field strengths the ionization probability is nearly unity. A closer examination shows that the minima are lower at $E_0 = 4$ a.u. than at $E_0 = 1.0$ a.u. This decrease in ionization probability with increasing field strength is an indication of stabilization, where the electron becomes more stable as the field strength is increased.

B. ATI spectrum and wave functions in scaled coordinates

For atoms in an intense laser field, once the time-dependent wave function is obtained, it can be used to calculate observable such as the harmonic generation spectrum and the ATI spectrum. The latter is done by simply projecting onto the continuum states. In Fig. 5, we show the ATI spectrum as a solid curve for $E_0 = 0.1$ a.u. and $\omega = 0.148$ a.u. for a laser that was turned off after 8.25 cps. Physically, the sharp peaks in the ATI spectrum indicate that there are ionized electrons with reasonably well-defined energies (or velocities). It is worthwhile to see whether this information can be seen directly in the wave function. To this end, we also show in Fig. 5 the probability density in the scaled coordinate after freely propagating the wave function from 8.25 to 80 cps.

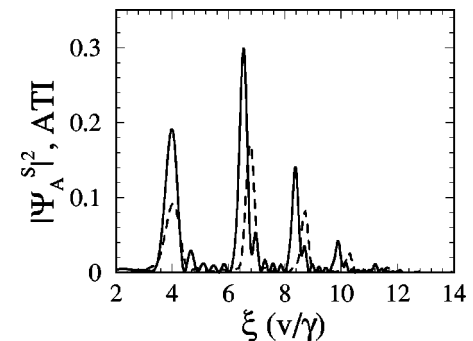


FIG. 5. Comparison of the position of the ATI peaks in scaled coordinates with the probability density at a large time. See text for the details of the parameters used in the calculation.

Note that the ATI spectrum is plotted vs v/γ with v the velocity of the electron (converted from its energy) and $\gamma = 0.1$ a.u. The first ATI peak coincides with the first peak of the density. For the higher peaks, the overlap is not as good, with the peak positions of the density distribution lagging behind the ATI peaks, but a one-to-one correspondence can be easily discerned. According to Eq. (11), a freely propagating Gaussian wave packet is stationary in the large time limit in scaled coordinates with the peak located at $\xi = k_0/\gamma$. Thus, each peak in the probability density is a wave packet representing a ‘‘burst’’ of ionized electrons whose velocity can be read directly from the position of the peak.

The shift of the probability density peaks with respect to the ATI peaks can be understood by realizing that each wave packet is created at a different characteristic time. Following through the scaling transformation with $R(t) = \sqrt{1 + 0.01(t - 50)^2}$, we find that the center of the wave packet in the scaled space is at

$$\frac{v(t - t_c)}{R} = \frac{v(t - t_c)}{\sqrt{1 + 0.01(t - 50)^2}}, \quad (22)$$

if the wave packet was created at time t_c and then propagated freely. At large time t ,

$$\frac{v(t - t_c)}{R} \rightarrow \frac{v(t - t_c)}{0.1(t - 50)} \approx \frac{v}{0.1} - \frac{t_c - 50}{t} \frac{v}{0.1}. \quad (23)$$

The deviation between the ATI peak and the density peak is thus expressed by the second term on the right. At a given time, the difference is proportional to the velocity of the electron in each ATI peak. Figure 5 indeed shows that the deviations are larger for the higher ATI peaks. To show that the deviation also has to do with the asymptotic time when the wave function is examined, we show in Fig. 6(a) the second ATI peak and the density of the wave function at 40, 80, and 120 cps, with the laser field turned off at 8.25 cps. One can see the deviations become smaller at the larger times. The density peak will presumably coincide with the ATI peak at infinitely large times.

From Eq. (23), the shift of the density peak from the ATI peak also depends on the formation time of the wave packet. In general, a longer pulse would have a larger average creation time. To see how this is reflected in the calculated wave function, Fig. 6(b) shows the density distributions of the wave functions at 80 T, in one case the laser was turned off at 6.25 T and in the other at 8.25 T. For the longer pulse, the density peak lags behind the ATI peak more since t_c in Eq. (23) is larger. We have checked that the difference in the shift in Fig. 6(b) is not due to the difference in the free propagation time and that the ATI peak positions calculated from the two pulses are identical.

The time-dependent wave function thus directly shows quite clearly ATI features. This result is not specific to the scaling method, but scaling makes calculating and observing these features considerably simpler. In particular, the wave function must evolve freely for a long time after the laser is turned off in order to see the simple structure in Fig. 5. This long evolution time is necessary to allow the wave packets

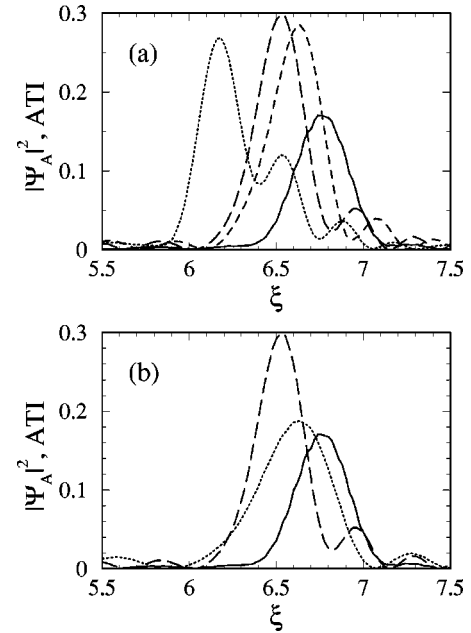


FIG. 6. (a) Comparison of the position of the second ATI peak with the nearby peak of the probability density at 40 T, 80 T, and 120 T for a laser pulse turned off at 8.25 T, showing that the peak in the wave function approaches the ATI peak asymptotically. (b) Comparison of the ATI peak and the probability density for two laser pulses at 80 T. The dashed lines are for a laser pulse turned off at 8.25 T, and the dotted lines are for a laser turned off at 6.25 T. The shift is a measure of the average time of the creation of the ATI peaks.

for each order of ATI generated at different times during the laser pulse to coalesce into a single wave packet. In the example above, for instance, the wave packet corresponding to the ATI peak might be composed of two wave packets, one created at the beginning of the laser pulse and the other at the end. Both of these wave packets have the same velocity, but are initially spatially and temporally separated. As time increases, the wave packets travel and spread. Eventually, they coalesce into a single wave packet spatially separate from the wave packets corresponding to other ATI peaks. At short times, then, the wave function is a complicated collection of several ionized wave packets overlapping and interfering. Propagation to long time allows the simple structure of Fig. 5 to emerge, and the scaling method makes this long time propagation especially simple. Returning to Fig. 5, we see that a grid in real space would have to range roughly from -4500 to 4500 a.u. with a maximum step size of 1 a.u. in order to include the momentum components necessary to represent the highest ATI peak, 9000 points would thus be needed while the present calculation was carried with 200 B splines.

IV. SUMMARY AND DISCUSSION

In this paper, we investigate the solution of the time-dependent Schrödinger equation of a one-dimensional atom in an intense laser field using scaled coordinates. Two of the fundamental problems of the time-dependent wave function

in coordinate space are the spreading and the rapid phase oscillation of the wave function at large times. The scaled coordinate removes both of these problems analytically. When atoms are exposed to an intense laser, additional oscillations on the wave function from the quiver motion of the laser field can be reduced by calculating the wave function in the KH frame, i.e., in the acceleration gauge. By combining the scaling and the acceleration gauge, we show that it is possible to perform accurate calculations for the one-dimensional soft-Coulomb problem in an intense laser field without using absorbers at the boundaries. We have calculated the total ionization rate and showed the wave function in the KH frame tends to be more localized as the field strength is increased. We further demonstrated that information on the ATI peaks can be seen directly in the wave func-

tions in the scaled coordinate if we let the wave function propagate freely over a long time. The scaled coordinate method is thus not only more convenient for the solution of the time-dependent Schrödinger equation, but allows simply for propagation to large times so that the ATI peaks can also be seen in the wave function itself. By greatly reducing the computational burden for laser-atom interactions, we hope to more easily treat fully three-dimensional problem.

ACKNOWLEDGMENT

This work is in part supported by Chemical Sciences, Geosciences and Biosciences Division, Office of Basic Energy Sciences, Office of Science, U.S. Department of Energy.

-
- [1] K. Burnett, V. C. Reed, and P. L. Knight, *J. Phys. B* **26**, 561 (1993); M. Protopapas, C. H. Keitel, and P. L. Knight, *Rep. Prog. Phys.* **60**, 389 (1997).
- [2] J. L. Hall, E. J. Robinson, and L. M. Branscomb, *Phys. Rev. Lett.* **14**, 1013 (1965).
- [3] L. V. Keldysh, *JETP* **47**, 1945 (1964) [*Sov. Phys. JETP* **20**, 1307 (1965)].
- [4] P. Agostini, F. Fabre, G. Mainfray, G. Petite, and N. K. Rahman, *Phys. Rev. Lett.* **42**, 1127 (1979).
- [5] P. Kruit, J. Kimman, H. G. Muller, and M. J. van der Wiel, *Phys. Rev. A* **28**, 248 (1983).
- [6] B. W. Shore and P. L. Knight, *J. Phys. B* **20**, 413 (1987).
- [7] A. L'Hullier and Ph. Balcou, *Phys. Rev. Lett.* **70**, 774 (1993).
- [8] S. I. Chu, *Adv. At. Mol. Phys.* **21**, 197 (1985).
- [9] R. M. Potvliege and R. Shakeshaft, *Phys. Rev. A* **38**, 4597 (1988).
- [10] P. G. Burke, P. Framcken, and C. J. Joachain, *J. Phys. B* **24**, 761 (1991).
- [11] S. Geltman, *J. Phys. B* **33**, 1967 (2000).
- [12] G. L. Kamta, T. Grisges, B. Piraux, R. Hasbani, E. Cormier, and H. Bachau, *J. Phys. B* **34**, 857 (2001).
- [13] L. A. Collins and A. L. Merts, *J. Opt. Soc. Am. B* **7**, 647 (1990).
- [14] T. Mercouris and C. A. Nicolaides, *J. Phys. B* **33**, 2095 (2000).
- [15] Xiaoxin Zhou and C. D. Lin, *Phys. Rev. A* **61**, 053411 (2000).
- [16] Q. Su, J. H. Eberly, and J. Javanainen, *Phys. Rev. Lett.* **64**, 862 (1990).
- [17] J. Javanainen, J. H. Eberly, and Q. Su, *Phys. Rev. A* **38**, 3430 (1988).
- [18] J. H. Eberly, Q. Su, and J. Javanainen, *J. Opt. Soc. Am. B* **7**, 1289 (1989).
- [19] V. C. Reed and K. Burnett, *Phys. Rev. A* **42**, 3152 (1990).
- [20] B. I. Schneider, *Phys. Rev. A* **55**, 3417 (1997).
- [21] M. Gavrilin and J. Shertzer, *Phys. Rev. A* **53**, 3431 (1996).
- [22] Jian Zhang and P. Lambropoulos, *Phys. Rev. Lett.* **77**, 2186 (1996).
- [23] E. Y. Sidky and C. D. Lin, *Phys. Rev. A* **60**, 377 (1999).
- [24] E. Y. Sidky and B. D. Esry, *Phys. Rev. Lett.* **85**, 5086 (2000).
- [25] L. I. Schiff, *Quantum Mechanics*, 3rd ed. (McGraw-Hill, New York, 1968), p. 63.